

OH(A-X) Fluorescence from Photodissociative Excitation  
of HO<sub>2</sub> at 157.5 nm

114113

219

M. Suto, C. Ye, M. J. Mitchell\*, and L. C. Lee\*\*  
Department of Electrical and Computer Engineering  
San Diego State University  
San Diego, CA 92182

Abstract

The OH(A-X) fluorescence from photodissociative excitation of HO<sub>2</sub> by F<sub>2</sub> laser photons (157.5 nm) was observed and compared with the OH fluorescence spectra of H<sub>2</sub>O<sub>2</sub> and the O<sub>2</sub>+CH<sub>3</sub>OH mixture. The rotational population distributions of OH(A) were obtained from the fluorescence spectra. The most populated levels are J=4 for photodissociative excitation of HO<sub>2</sub>, J=20 for H<sub>2</sub>O<sub>2</sub>, and J=21 for the O<sub>2</sub>+CH<sub>3</sub>OH mixture. The fluorescence from the gas mixture is attributed to the O+H recombination for which the atoms are produced from photodissociation of parent molecules.

(NASA-CR-181580) OH(A-X) FLUORESCENCE FROM  
PHOTODISSOCIATIVE EXCITATION OF HO<sub>2</sub> AT 157.5  
nm (San Diego State Univ.) 19 p Avail:  
NTIS HC A03/MF A01

N88-13429

CSCL 07D

Unclass

G3/25 0114113

\* Present address: Department of Chemistry, University of  
Houston, University Park, Houston, TX 77004

\*\* Also, Department of Chemistry, San Diego State University

## I. Introduction

HO<sub>2</sub> is important in the study of atmospheric and combustion chemistry. Optical detection method is interested for monitoring HO<sub>2</sub> in various environments. It is demonstrated that HO<sub>2</sub> can be detected by photofragment emissions.<sup>1-4</sup> Excitation of HO<sub>2</sub> at 193 and 248 nm produces O(<sup>1</sup>D), which then transfers energy to O<sub>2</sub> to produce the O<sub>2</sub> (b → a) emission.<sup>1</sup> Photoexcitation of HO<sub>2</sub> at 121.6, 123.6 and 147 nm produces the OH(A-X) fluorescence.<sup>2,3</sup> This OH fluorescence has been used as a means to detect HO<sub>2</sub> for kinetic measurements.<sup>3,4</sup>

In the early studies,<sup>2-4</sup> the OH fluorescence intensity produced by a atomic resonance line was too weak to be dispersed. In this experiment, F<sub>2</sub> laser at 157.5 nm was used as a light source. The fluorescence intensity is so strong that it can be dispersed. The OH(A-X) fluorescence spectrum from HO<sub>2</sub> was compared with that of H<sub>2</sub>O<sub>2</sub> observed in the same experiment. Their fluorescence spectra are so different that these two molecules can be distinctly detected by their photofragment emissions.

The HO<sub>2</sub> radicals were produced by either the three-body recombination process,



or by the sequential reactions,



During the study of using the sequential reactions as the HO<sub>2</sub> source, it was found that additional OH fluorescence was produced from the laser excitation of the O<sub>2</sub> + CH<sub>3</sub>OH mixture alone (without HO<sub>2</sub>). The fluorescence is produced from the O+H recombination, where the atoms are produced from photodissociation of O<sub>2</sub> and CH<sub>3</sub>OH. The observation of this emission system is also reported in this paper.

## II. Experiment

The experiment for the production of HO<sub>2</sub> by reaction (1) has been described in detail in previous papers.<sup>1,2</sup> In brief, the H atom was produced by microwave discharge of a trace H<sub>2</sub> in He. O<sub>2</sub> was added to the H/H<sub>2</sub>/He flow to form HO<sub>2</sub> in the flow tube. HO<sub>2</sub> was irradiated by laser beam in the central region of gas cell in a direction perpendicular to the flow tube. The second method for the production of HO<sub>2</sub> by reactions (2) and (3) was also described in previous papers.<sup>3,4</sup> The Cl atom was produced by microwave discharge of a trace Cl<sub>2</sub> in He. Cl reacted with CH<sub>3</sub>OH and then O<sub>2</sub> to form HO<sub>2</sub> in the flow tube.

The laser intensity was monitored by a copper diode. Fluorescence was dispersed by a 0.25-m monochromator (Acton) and detected by a cooled photomultiplier tube (PMT EMI 9558 QB). The signal from the PMT was processed simultaneously by a gated photon counting system (EG&G ORTEC) and a boxcar integrator (EG&G, PAR162). The gates were opened for a period of 4  $\mu$ s after each laser pulse. The laser was operated at a repetition rate of 20 Hz and a pulse duration of 6 ns. The fluorescence spectra

were also monitored by a gated optical multichannel analyzer (EG&G, PAR, OMA III). Spectra taken by these different instruments are all similar.

### III. Results and Discussion

#### A. Fluorescence Spectra

A typical spectrum obtained from photoexcitation of  $\text{HO}_2$  is shown in Fig. 1a, where  $\text{HO}_2$  was produced by reaction (1). The fluorescence spectrum is identified as the  $\text{OH}(A, v'=0 \rightarrow X, v''=0)$  system. The fluorescence intensity was measured as a function of  $[\text{H}]$ ,  $[\text{O}_2]$ , and reaction time, for which the results are very similar to those described in the previous paper.<sup>2</sup> The fluorescence intensity depends linearly on the laser intensity (see Fig. 2), indicating that the fluorescence is produced by a single photon dissociative process.

$\text{H}_2\text{O}_2$  could be produced from the  $\text{HO}_2 + \text{HO}_2$  reaction in the flow tube, when  $[\text{HO}_2]$  is high. Photodissociation of  $\text{H}_2\text{O}_2$  at excitation wavelengths shorter than 172 nm will yield the  $\text{OH}(A-X)$  emission.<sup>5</sup> The cross section for the production of OH fluorescence from  $\text{H}_2\text{O}_2$  is  $9.2 \times 10^{-19} \text{ cm}^2$  at 157.5 nm.<sup>5</sup> The possible interference of the observed fluorescence by fluorescence from  $\text{H}_2\text{O}_2$  has been discussed in a previous paper.<sup>3</sup> It was concluded that the interference is not significant in the current discharge-flow-tube system.<sup>3</sup> Nevertheless, a check of this assertion by comparing the fluorescence spectra of these two chemical species is of interest.

The OH spectrum obtained from photoexcitation of H<sub>2</sub>O<sub>2</sub> at 157.5 nm in the presence of additive gasses (He, O<sub>2</sub>, and H<sub>2</sub>) is shown in Fig. 1b, where the additive gases were kept at the same partial pressures as those used in the HO<sub>2</sub> experiment so that the possible quenching effect of additive gases on the fluorescence spectrum is the same for both cases. The spectral envelopes of the OH emission spectra observed at various partial additive gas pressures were essentially the same, although the fluorescence intensity was reduced by the additive gases. As shown in Figs. 1a and 1b, the OH fluorescence spectral envelope of HO<sub>2</sub> is different from that of H<sub>2</sub>O<sub>2</sub>. The fluorescence spectra are used to derive rotational populations as discussed in the next section.

HO<sub>2</sub> was also produced by the reactions (2) and (3) in this experiment. When the mixture of HO<sub>2</sub> with O<sub>2</sub>, CH<sub>3</sub>OH, Cl<sub>2</sub>, HCl, and He was irradiated by F<sub>2</sub> laser photons, a fluorescence spectrum similar to Fig. 1b was observed. This spectrum is different from Fig. 1a that is expected for HO<sub>2</sub>. The spectral shape varies with gas concentration and laser flux. Later, it was found that laser irradiation of the O<sub>2</sub>+CH<sub>3</sub>OH gas mixture alone produces a fluorescence spectrum as shown in Fig. 1c. Similar spectra were also observed from laser irradiation of the gas mixtures of HCl+O<sub>2</sub> and H<sub>2</sub>O+O<sub>2</sub>. These results suggest that the fluorescence is produced by the O+H recombination. The O atom is produced from photodissociation of O<sub>2</sub> by the process,



At 157.5 nm, the quantum yield<sup>6</sup> for this process is about 1. The H atom is produced from photodissociation of CH<sub>3</sub>OH, HCl, or H<sub>2</sub>O. These molecules have high photoabsorption cross sections at 157.5 nm.<sup>7-9</sup>

The assertion that Fig. 1c results from the O+H recombination is further examined by the dependence of fluorescence intensity on laser flux as shown in Fig. 2a. Since [O] or [H] is linearly dependent on laser flux, the fluorescence intensity, which is proportional to [O] [H], depends on the square of laser energy,  $I^2$ . As shown in Fig. 2a, the intensities for both the first peak at 310 nm and the second peak at 315 nm can be fit by  $I^n$  with  $n=2$ . This square power dependence supports the assertion that the fluorescence is produced by the atomic recombination.

When HO<sub>2</sub> is produced by reactions (2) and (3), it always mixes with O<sub>2</sub> and CH<sub>3</sub>OH. More fluorescence signal was observed when the microwave discharge of Cl<sub>2</sub>/He was turned on, indicating that additional fluorescence was produced from the HO<sub>2</sub> photolysis. Since both the HO<sub>2</sub> photolysis and the O+H recombination contribute to fluorescence, the fluorescence intensity is proportional to  $aI + bI^2$ , where  $a$  and  $b$  depend on the concentrations of HO<sub>2</sub>, O<sub>2</sub>, and CH<sub>3</sub>OH. Since the HO<sub>2</sub> photolysis produces a high fluorescence intensity at the first band (310 nm, see Fig. 1(a)), the laser power dependence of this band intensity will be close to  $I^n$  with  $n \approx 1$ . On the other hand, the HO<sub>2</sub> fluorescence has a small intensity at the second band

(315 nm) so that  $n \approx 2$ . This expectation is consistent with the data as shown in Fig. 2b, where  $n=1.2$  for the first band and  $n=1.7$  for the second band.

The laser flux dependence of the fluorescence intensity from  $\text{HO}_2$  photolysis is also shown in Fig. 2b for comparison, where  $\text{HO}_2$  was produced from reaction (1). The  $n$  value is 1.05, indicating that the fluorescence is produced by a single-photon process. The partial contribution from the  $\text{O}+\text{H}$  recombination makes the  $n$  value slightly higher than 1. Since small amount of  $\text{H}_2\text{O}$  exists in the  $\text{H}/\text{H}_2/\text{O}_2$  system<sup>2</sup>, photodissociation of  $\text{H}_2\text{O}$  and  $\text{O}_2$  will produce the  $\text{OH}$  fluorescence by the recombination process.

#### B. Rotational Populations

A numerical model has been developed to simulate the  $\text{OH}(A, v'=0-X, v''=0)$  rovibrational spectra in the 300-340 nm region. Hund's case b was assumed, and discrete emission lines were calculated for all 12 branches. Wavelengths were calculated using the upper and lower energy levels taken from Dieke and Crosswhite;<sup>10</sup> line intensities were obtained using Einstein A coefficients as reported by Dimpfl and Kinsey.<sup>11</sup> The calculated lines were then broadened using a simulated slit with consisting of a simple triangular function with variable width (0.3-1.2 nm). Rotational populations of the  $\text{OH}(A)$  state were assumed to be non-thermal and non-Boltzmann in distribution, and were determined by the simulation as discussed below.

The resulting broadened spectral lines formed a spectral envelope that could be compared to the observed data shown in

Fig. 1 by a simple reduced chi-squared function. A non-linear, least squares minimization routine was developed from an algorithm discussed by Bevington.<sup>12</sup> This minimization routine was applied to the chi-squared fits of synthetic and actual spectra to obtain relative rotational populations of the OH(A,  $v'=0$ ) state.

The rotational distribution of OH(A) from the H<sub>2</sub>O<sub>2</sub> photolysis at 157.5 nm has been studied by Golzenleuchter et al.<sup>13</sup> They reported non-thermal rotational distribution with a maximum population at  $N'=21$  level. This study serves as a reference for the current simulation; thus, we started the synthetic calculation with the OH fluorescence from H<sub>2</sub>O<sub>2</sub> photolysis as shown in Fig. 1b. The least squares fit synthetic spectrum at a simulated resolution of 0.6 nm (width at half-height of triangular function) is shown in Fig. 1b to compare with the fluorescence spectrum which was taken at a monochromator resolution of 0.4 nm. (The difference between the simulated resolution and the monochromator resolution may be caused by the slit functions being different). The fitted spectrum was created by allowing the rotational population of OH(A) varying in the range of 0-27 levels. As can be seen, the fitted and actual spectra agree quite closely, particularly with regard to the overall shape. The relative rotational population distribution of the OH(A,  $v'=0$ ) state obtained from fitting the data of Fig. 1b is shown in Fig. 3 (triangle). The current population closely resembles the result of Golzenleuchter et al.<sup>13</sup> who analyzed the



Q<sub>2</sub> and P<sub>2</sub> branches with a maximum population at rotational level 21 and no population above level 26. The result of Golzenleuchter et al.<sup>13</sup> showed that about 97% of the observed OH emission arises from the  $v'=0$  vibrational level. The result from our extended model simulation that includes the  $v'=1$  level agrees with the earlier result. The rovibrational OH emission spectra produced from photodissociative excitation of H<sub>2</sub>O<sub>2</sub> can be well modeled by assuming that the  $v'=0$  to  $v''=0$  transition dominates. This agreement also indicates that the fluorescence spectrum is not affected by the additive gases used in the current experiment.

Using the same fitting procedure, the synthetic spectrum was calculated to compare with the OH fluorescence spectrum produced from photolysis of HO<sub>2</sub> as shown in Fig. 1a. The fitted synthetic spectrum shown in Fig. 1a was obtained at a simulated slit width of 1.0 nm (again this is higher than the monochromator resolution of 0.6 nm). The intensity of the observed OH fluorescence was low and thus somewhat noisy; therefore, no attempt was made to fit any of the finer structural features. As can be readily seen from Fig. 1a, the fit of the overall peak envelope is good for wavelengths to the blue side of about 312 nm and increasingly poor towards the red end. The fitted spectrum was restricted to include contribution from only the lower 16 rotational levels as there is a constraint of available energy for the rotational population. The available energy for photodissociation of HO<sub>2</sub> at 157.5 nm into OH(A,  $v'=0$ ) + O (<sup>3</sup>P) is 0.89 eV and that of H<sub>2</sub>O<sub>2</sub>

into  $\text{OH}(A, v'=0) + \text{OH}(X)$  is 1.64 eV, as calculated from the electronic energy of  $\text{OH}(A, v'=0) = 4.017 \text{ eV}^{14}$  and the heats of formation<sup>15</sup> of 2.09, 38.987, 249.17 and -136.106 kJ/mol for  $\text{HO}_2$ , OH, O, and  $\text{H}_2\text{O}_2$ , respectively. The available energy is sufficient to populate the rotational level up to  $J=28$  for  $\text{OH}(A, v'=0)$  from photolysis of  $\text{H}_2\text{O}_2$ , and  $J=20$  for that of  $\text{HO}_2$ . Since the rotational populations at  $J \leq 26$  for  $\text{H}_2\text{O}_2$  (see Fig. 3), it is assumed, in analogy, that  $J \leq 16$  for  $\text{HO}_2$ . The rotational distribution for the synthetic spectrum of Fig 1a is shown in Fig.3 (circle). The population has a maximum at  $J=4$ , which is significantly lower than that of  $\text{H}_2\text{O}_2$ .

For the second band (315 nm), the intensity of the observed spectrum is higher than that of the synthetic spectrum. The additional observed signal may indicate that there is a contribution from the  $\text{O}+\text{H}$  recombination which has a large intensity at the second band. The dependence of fluorescence intensity on laser flux also indicates this contribution as discussed before.

The comparison of the synthetic spectrum with the fluorescence spectrum of the  $\text{O}_2 + \text{CH}_3\text{OH}$  mixture is shown in Fig. 1c. The population corresponding to the synthetic spectrum is shown in Fig. 3 (square). The overall shape of the emission envelope is fairly well modeled by the fitted and smoothed population distribution, except for the sharp feature at  $\sim 312 \text{ nm}$  which is not well modeled and may arise from the  $\text{OH}(A, v'=1 \rightarrow X, v''=1)$  transition. The fitted population distribution exhibits

a maximum at rotational level 21 as might be expected from the similarity in the shapes of the spectral envelopes of Figs. 1b and 1c. The OH (A,  $v'=0$ ) populations arising from the H+O reaction or from the H<sub>2</sub>O<sub>2</sub> photoexcitation have a similar non-Boltzmann rotational distribution.

The OH(A<sup>2</sup> $\Sigma^+$ ) state could be produced from the recombination of O(<sup>1</sup>D) + H(<sup>2</sup>S) which is correlated<sup>16</sup> with the A state, and/or from the recombination of O(<sup>3</sup>P)+H(<sup>2</sup>S) through the <sup>4</sup> $\Sigma^-$  state.<sup>17-20</sup> Both O(<sup>1</sup>D) and O(<sup>3</sup>P) are produced by photodissociation<sup>6</sup> of O<sub>2</sub> by the process (4) with a kinetic energy of 0.39 eV for each atom. This kinetic energy is sufficient for the recombination of O(<sup>3</sup>P) + H(<sup>2</sup>S) through the  $v=2$  level of the OH(A) state. The populations in high vibrational levels that are possibly produced by the O(<sup>1</sup>D) + H(<sup>2</sup>S) recombination are largely predissociated by the <sup>4</sup> $\Sigma^-$  state.<sup>17-20</sup> Thus, only emission from the  $v=0$  and 1 vibrational levels are mostly observed. The rotational levels higher than  $J=27$  are strongly predissociated.<sup>19</sup> The rotational population distribution shown in Fig. 3 is consistent within these physical constraints.

### Conclusion

The OH(A-X) fluorescence spectra produced from photolysis of HO<sub>2</sub>, H<sub>2</sub>O<sub>2</sub>, and the O<sub>2</sub> + CH<sub>3</sub>OH mixture at 157.5 nm were observed and used to derive the rotational distributions of OH (A, v'=0). The OH(A, v'=0) produced from photolysis of HO<sub>2</sub> is populated in the rotational levels much lower than that of H<sub>2</sub>O<sub>2</sub>. This result suggests that HO<sub>2</sub> and H<sub>2</sub>O<sub>2</sub> can be distinctly detected by the different OH fluorescence spectra.

### Acknowledgement

This report is based on the work supported by Grants from the NSF and the NASA.

### References

1. L. C. Lee, J. Chem. Phys. 76, 4909 (1982).
2. M. Suto and L. C. Lee, J. Chem Phys. 80, 195 (1984).
3. W. C. Wang, M. Suto and L. C. Lee, J. Chem. Phys. 81, 3122 (1984).
4. E. R. Manzanares, M. Suto, L. C. Lee and D. Coffey Jr., J. Chem. Phys. 85, 5027 (1986).
5. M. Suto and L. C. Lee, Chem. Phys. Lett. 98, 152 (1983).
6. L. C. Lee, T. G. Slanger, G. Black, and R. L. Sharpless, J. Chem. Phys. 67, 5602 (1977).
7. J. B. Nee, M. Suto and L. C. Lee, Chem. Phys. 98, 147 (1985).
8. J. B. Nee, M. Suto and L. C. Lee, J. Chem. Phys. 85, 719 (1986).
9. L. C. Lee and M. Suto, Chem Phys. 110, 161 (1986).
10. G. H. Dieke and H. M. Crosswhite, J. Quant. Spectrosc. Radiat. Transfer, 2, 97 (1961).
11. W. L. Dimpfl, and J. L. Kinsey, J. Quant. Spectrosc. Radiat. Transfer, 21, 233 (1979).
12. P. R. Bevington, Data Reduction and Error Analysis for the Physical Sciences (McGraw-Hill, New York 1969).
13. H. Golzenleuchter, H. -H. Gericke, F. J. Comes and P. F. Linde, Chem. Phys. 89, 93 (1984).
14. K. P. Huber and G. Herzberg, "Constants of Diatomic Molecules" (Van Nostrand, Princeton, 1979).

15. M. W. Chase, Jr., C. A. Davies, J. R. Downey, Jr., D. J. Frurip, R. A. McDonald, and A. N. Syverad, JANAF Thermochemical Tables, Third Edition, J. Phys. Chem. Ref. Data, Vol. 14, Suppl. No. 1, (1985).
16. S. Ticktin, G. Spindler, and H. Schiff, Disc. Farad. Soc. 44, 218 (1967).
17. K. R. German, J. Chem. Phys. 63, 5252 (1975).
18. T. Bergeman, P. Erman and M. Larsson, Chem. Phys. 54, 55 (1980).
19. M. L. Sink, A. D. Bandrauk, and R. Lefebvre, J. Chem. Phys. 73, 4451 (1980).
20. H. B. Palmer and D. W. Naegli, J. Chem. Phys. 59, 994 (1973).

### Figure Captions

Fig. 1. OH(A-X) fluorescence spectra (—) and synthetic spectra (---). (a) Fluorescence from laser photolysis of HO<sub>2</sub> taken at a monochromator resolution of 0.6 nm. HO<sub>2</sub> was produced by a microwave discharge of 3 mtorr H<sub>2</sub> in 8.5 torr He which then reacted with 50 mtorr O<sub>2</sub> added downstream for a reaction time of 0.28 sec. (b) Laser photolysis of H<sub>2</sub>O<sub>2</sub> taken at 0.4 nm resolution. Gases were added to flow tube to keep the experimental condition to be the same as (a), except that the microwave discharge was turned off. (c) Laser photolysis of the O<sub>2</sub>/CH<sub>3</sub>OH/He gas mixture with partial pressures of 20/3/3000 mtorr, respectively. The spectrum was taken at a monochromator resolution of 0.8 nm.

Fig. 2. Dependence of fluorescence intensity ( $I_f$ ) on laser flux ( $I$ ). The data were fitted by  $I_f \propto I^n$ . (a) Fluorescence from laser photolysis of the O<sub>2</sub>+CH<sub>3</sub>OH mixture measured at the band peaks of 310 and 315 nm. The partial pressures of O<sub>2</sub>/CH<sub>3</sub>OH/He were 20/5/500 mtorr. (b) Fluorescence from laser photolysis of the HO<sub>2</sub>+O<sub>2</sub>+CH<sub>3</sub>OH gas mixture. HO<sub>2</sub> was produced by a microwave discharge of 3 mtorr Cl<sub>2</sub> in 500 mtorr He with 8 mtorr O<sub>2</sub> and 0.3 mtorr CH<sub>3</sub>OH added downstream. The fluorescences were observed at 310 (▲) and 315 (●) nm. The fluorescence from laser photolysis of HO<sub>2</sub> was also

plotted for comparison, where HO<sub>2</sub> was produced by a microwave discharge of 3 mtorr H<sub>2</sub> in 6 torr He with 60 mtorr O<sub>2</sub> added downstream.

Fig. 3. Relative rotational population of OH(A, v'=0) derived from the synthetic spectra shown in Figs. 1a (●), 1b (▲), and 1c (■).



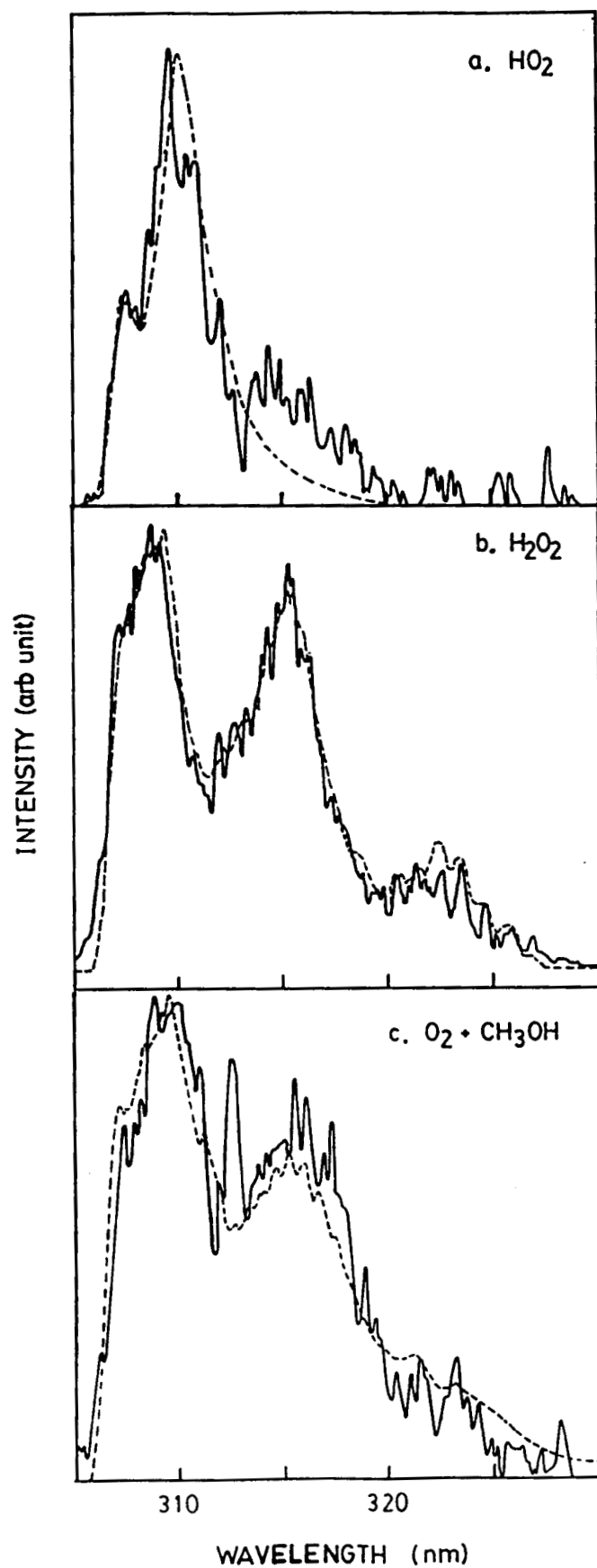


Fig. 1

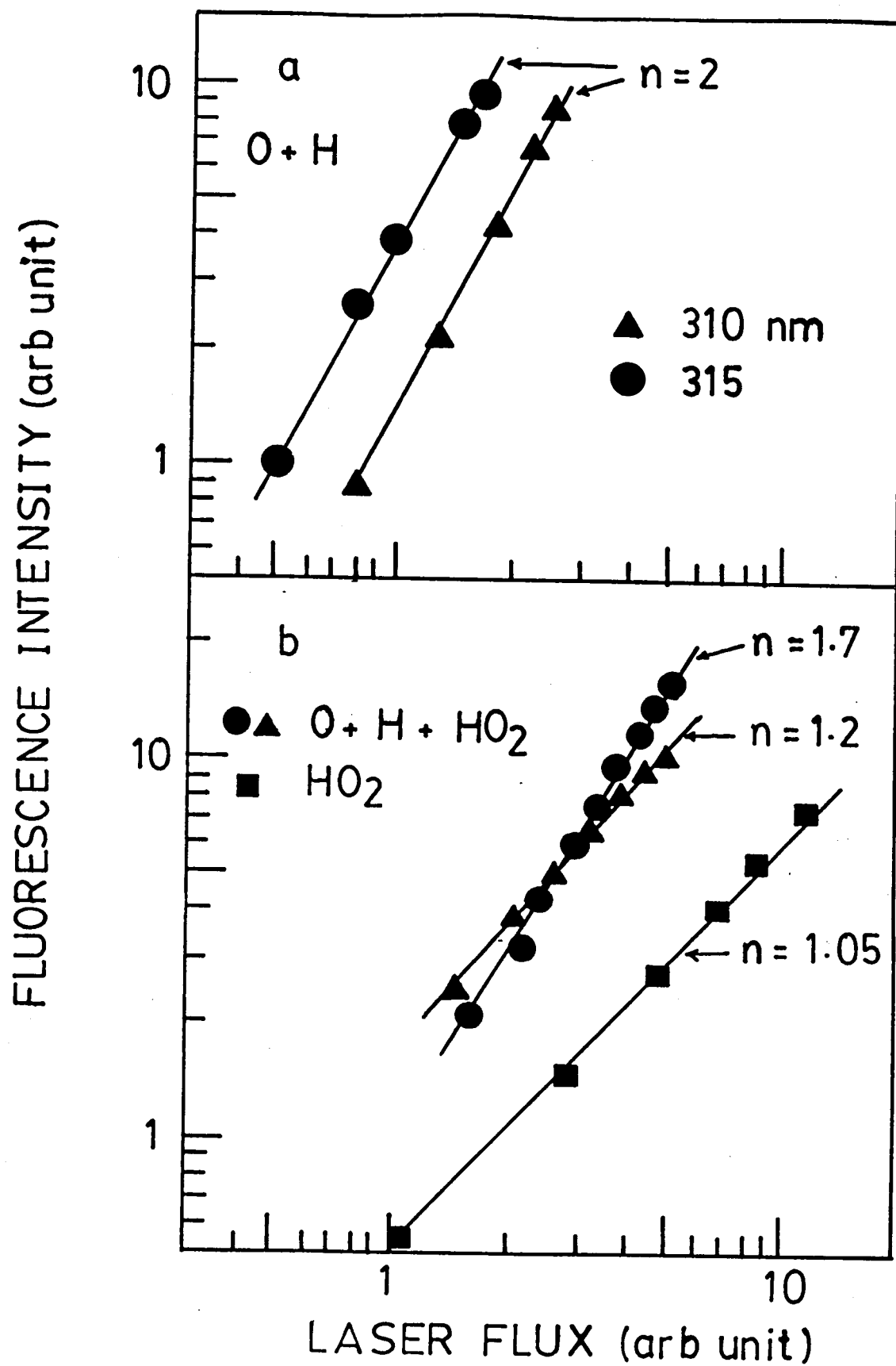


Fig. 2

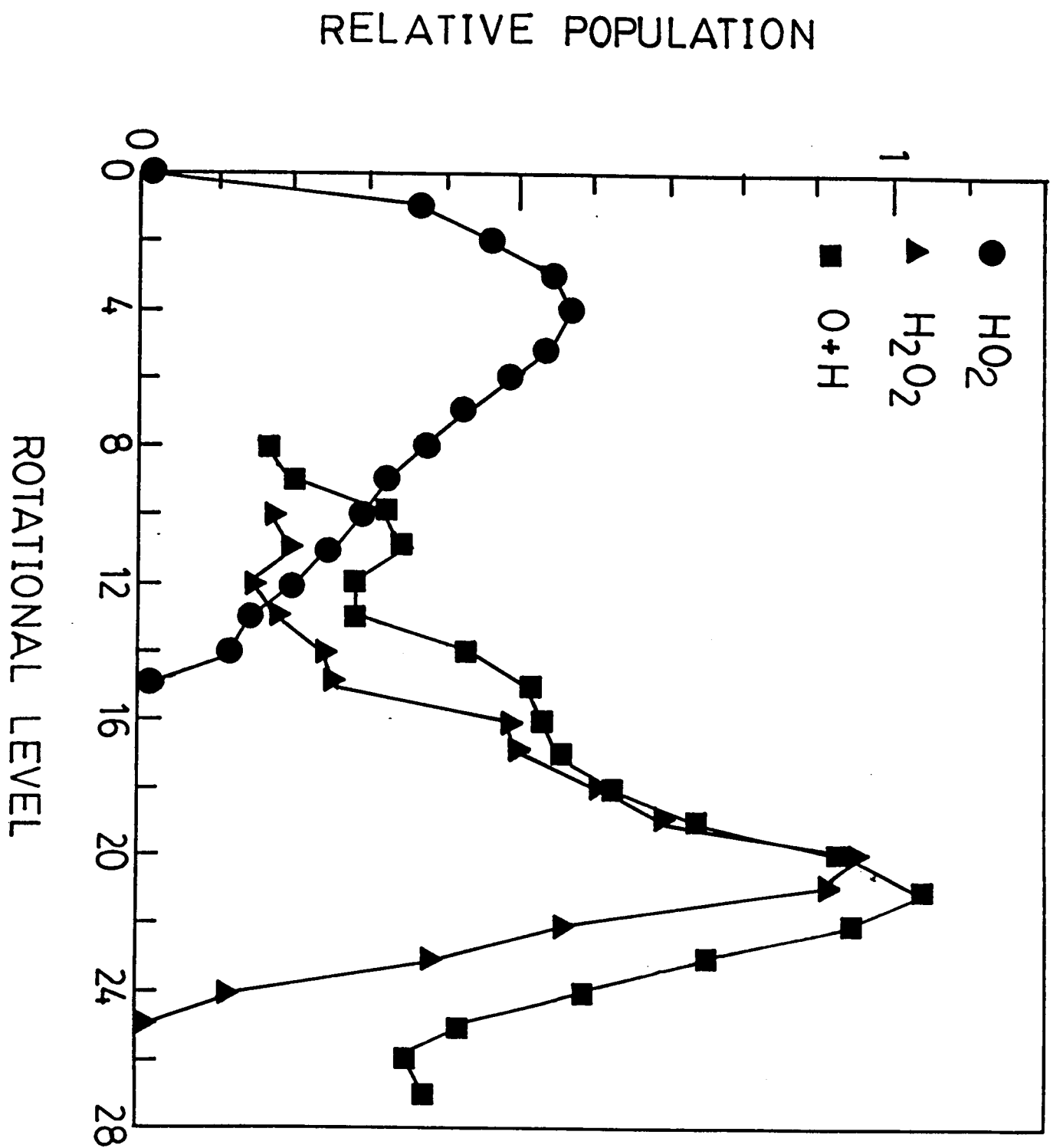


Fig. 3.